Bio-inspired signal transduction with heterogeneous networks of nanoscillators

Javier Cervera, José A. Manzanares, and Salvador Mafé

Citation: Appl. Phys. Lett. **100**, 093703 (2012); doi: 10.1063/1.3691630
View online: http://dx.doi.org/10.1063/1.3691630
View Table of Contents: http://apl.aip.org/resource/1/APPLAB/v100/i9
Published by the American Institute of Physics.

Bio-inspired signal transduction with heterogeneous networks of nanoscillators

Javier Cervera, José A. Manzanares, and Salvador Mafé[a)]
Facultat de Física, Universitat de València, E-46100 Burjassot, Spain

(Received 16 January 2012; accepted 14 February 2012; published online 2 March 2012)

Networks of single-electron transistors mimic some of the essential properties of neuron populations, because weak electrical signals trigger network oscillations with a frequency proportional to the input signal. Input potentials representing the pixel gray level of a grayscale image can then be converted into rhythms and the image can be recovered from these rhythms. Networks of non-identical nanoscillators complete the noisy transduction more reliably than identical ones. These results are important for signal processing schemes and could support recent studies suggesting that neuronal variability enhances the processing of biological information. © *2012 American Institute of Physics*. [http://dx.doi.org/10.1063/1.3691630]

Weak signals, noise, and significant variability between nominally identical hardware components are inherent to nanoelectronics. This variability may be undesirable for most applications: the threshold voltage mismatching of individual electronic transistors can have profound effects in voltage-driven applications.[1] In contrast, natural variability can make noisy biological circuits to function more efficiently because non-identical nanostructures are integrated in summing networks.[2–4] Simulations concerning the role and function of noise and neural heterogeneity in the integrated population response of the vestibulo-ocular reflex showed that a heterogeneous population where each member displays a different rate of spontaneous activity produces a response with higher fidelity than a homogeneous population.[2,3] While neuronal noise was originally considered a biological limitation, it has been shown to provide a wide range of different spiking behaviors useful for coding in neuronal populations.[4–6] Thus, intrinsic neuronal diversity can be useful and not the result of natural imprecision.[4,5]

Frequency-based signal processing is inherent to brain functions. The transduction of external information into patterns of neural activity occurs in the presence of neuronal noise and discernible rhythms are characteristic of the behavioral and perceptual brain states. The models that describe how neural spike trains convey sensory information are relatively complex and include sophisticated decoding methods for reading out the information contained in the neural responses.[7,8] Simple models that can mimic some of the essential properties of neurons are useful for qualitative purposes. The threshold behavior of single-electron transistors is reminiscent of the gating process in integrate-and-fire neuron models. Simulations of pulse-density modulation with a heterogeneous ensemble of single-electron circuits showed that heterogeneity in the device parameters improves the reliability with which the neurons can encode signals of high input frequencies.[9] Recent experimental studies on a parallel network of GaAs-based nanowire field-effect transistors with different threshold voltages have shown that a network operating in the sub-threshold region can detect weak signals in the presence of noise.[10] The dynamic range of the system widens due to the threshold variability and the output summation process. While applications to image processing were suggested,[11] the individual units in the network did not show any oscillatory behavior.

Biological diversity and nanostructure variability can be useful for signal transduction and processing. When trying to design nanodevices, the fabrication uncertainties lead to a high variability in the properties of the individual nanostructures.[12,13] *Could this variability be exploited in the design of information processing schemes?* We show here that signal transduction applications can take advantage of this variability by exploiting some of the characteristics of biological systems. Nanoparticle (NP)-based organic transistors have been used as models for biological spiking synapses in neural networks and they are considered as basic units for neuromorphic circuits.[9,14–16] The different shape and size distributions of nanoparticles[13] result in a significant variability in their threshold potentials. Kinetic Monte Carlo simulations with these nanostructures have recently shown that moderate redundancy decreases the adverse effects of this variability and enhances the processing of weak, sub-threshold signals by taking advantage of the threshold fluctuations.[12,15]

Parallel arrays of resistance-single electron transistors (R-SETs) can be used for frequency-based image processing. The equivalent circuit of the SET consists of a capacitance C_i arranged in parallel to a resistance R_i.[13,14,21] The resistance r_i is connected in series to the SET to complete the R-SET. This system can be realized experimentally by means of ligand-stabilized metallic nanoparticles.[17–23] The nanoparticle is functionalized with an organic ligand acting as a tunneling junction, so that the electron transfer from the NP to the electrode is based on Coulomb blockade and tunneling.[17–23] The functionalized NPs behave as multivalent redox species with charge states separated by approximately constant energy differences. The single electron transfers to and from the NP lead to measurable electric potential changes of the order of 100 mV that give effective capacitances of the order of 1 aF.[19–24] For example, the electrochemically determined capacitance[19] of Au_{225} NPs with a diameter of 1.8 nm is ca. 0.6 aF and smaller particles like Pd_{40} (1.2 nm diameter) show a capacitance of ca. 0.35 aF.

[a)]Author to whom correspondence should be addressed. Electronic mail: smafe@uv.es.

The current–voltage curves of a single ligand-stabilized NP obtained by scanning tunneling spectroscopy can also be fitted to theoretical SET models based on equivalent circuits to obtain the effective electrical parameters.[21,23,25] In this case, the typical values found for the tunneling resistances and capacitances are usually in the range of 10 MΩ–1 GΩ and 0.1–5 aF, respectively.[18–25]

A potential $V_0 > 0$ applied to the i-th NP (Fig. 1(a)) through a resistance $r_i \gg R_i$ increases the NP potential $V_i(t)$ due to the charging process described by the differential equation $r_i C_i \mathrm{d}V_i/\mathrm{d}t = V_0 - V_i$.[14,15] The natural variability in the electrical parameters of the nanostructures is taken into account by considering a distribution of the individual capacitances C_i (Fig. 1(b)) such that $1 - \delta \leq C_i/C \leq 1 + \delta$, where $C = 1$ aF is the central value and δ is the relative variability.[13,14] This gives an average threshold potential[14,15] $V_{\mathrm{th}} = e/(2C) \approx 80$ mV. The resistances R_i and r_i have distributions of the same δ around the central values[21,23] $R = 50$ MΩ and $r = 1$ GΩ. The central values of C and R are realistic estimates obtained from the available experimental data.[18–25] The choice of r follows from the requirement $r_i \gg R_i$.

When V_0 exceeds the threshold potential $V_{\mathrm{th},i} = e/(2C_i)$ of the i-th NP, where e is the elementary charge, the NP potential $V_i(t)$ increases until it reaches $V_{\mathrm{th},i}$ and then an electron tunnels from the ground to the NP across the tunneling junction (see Fig. 1(a)). This makes $V_i(t)$ to decrease abruptly to $-V_{\mathrm{th},i}$. The variability in the electrical parameters of the nanostructures yields statistical distributions for the threshold potentials $V_{\mathrm{th},i}$ and the relaxation times $r_i C_i$ similar to that of Fig. 1(b). The charging-tunneling process produces relaxation oscillations that mimic oscillatory phenomena in biological networks of threshold units.[7] The oscillations are reminiscent of the firing events (spikes) in integrate-and-fire neurons[9] (see Fig. 1(c)). The period of the oscillations is approximately the time it takes for $V_i(t)$ to rise from $-V_{\mathrm{th},i}$ to $+V_{\mathrm{th},i}$. This time depends not only on the individual relaxation times $r_i C_i$ but also on the applied potential V_0 (Fig. 1(c)).

The threshold and relaxation time variability of the nanoscillators can be viewed as a static noise to be added to the dynamic noise produced by the thermally assisted tunneling events. According to the semi-classical orthodox theory,[15] the electron tunneling rate between the right electrode and the NP of Fig. 1(a) is described by the equations

$$\Gamma_i^{\rightleftarrows} = \frac{1}{eR_i^2} \frac{-\Delta E_i^{\rightleftarrows}}{1 - \exp(\Delta E_i^{\rightleftarrows}/kT)},$$

where k is Boltzmann's constant, T is the absolute temperature, and

$$\Delta E_i^{\rightleftarrows} = \mp e\left[V_{\mathrm{th},i}(1 + 2n_i) - V_0\right]$$

is the electrostatic energy change when the electron is transferred from the NP to the ground electrode (→) and from the ground electrode to the NP (←). In Eq. (2), n_i is the electronic occupancy of the NP (the excess or defect number of electrons). Figure 1(c) shows that, because of the finite temperature $T = 5$ K, an electron may tunnel before $V_i(t)$ reaches the threshold value $V_{\mathrm{th},i}$. Multiple tunneling events from the NP to the electrode and from the electrode to the NP may occur when $V_i(t)$ is close to $V_{\mathrm{th},i}$ (see Fig. 1(c)). Nonetheless, the net effect is the periodic tunneling of an electron from the ground electrode to the NP.

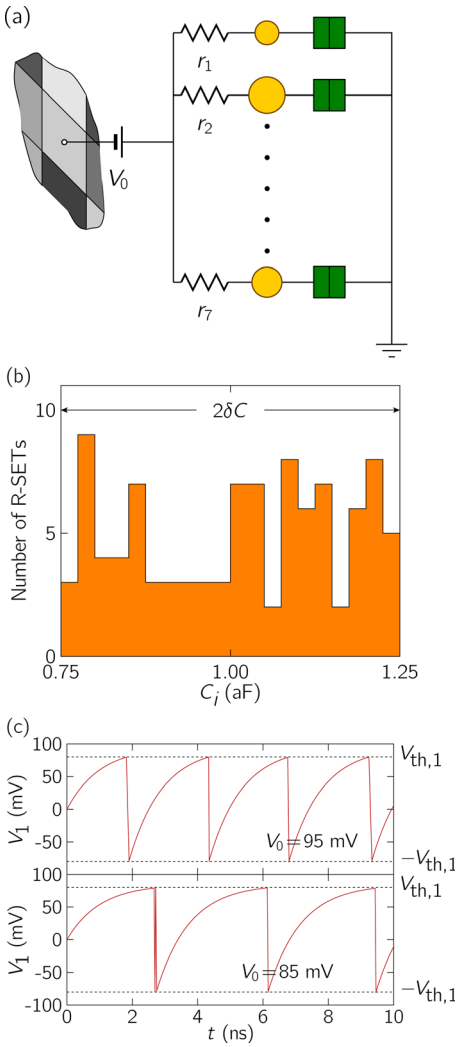

FIG. 1. (Color online) (a) Scheme of a parallel network of N R-SETs individually composed of a NP connected in series to a tunneling junction. The equivalent circuit of the NP and its tunneling junction (not shown) consists of a capacitance C_i arranged in parallel to a resistance R_i.[13,14,21] The potential V_0 applied to this network is a linear function of the pixel gray level in an 8-bit grayscale digital image. (b) A randomly generated distribution for the individual capacitances C_i of $N = 100$ R-SETs with relative variability $\delta = 0.25$ and the central value $C = 1$ aF. (c) Individual oscillatory charge-tunneling processes (spikes) occur when a potential V_0 is applied, as shown here for the NP potential of $i = 1$ R-SET.

The network oscillations have been simulated using a mixed continuum-Monte Carlo approach previously described.[14,15] The results shown in Fig. 2 correspond to the average values obtained from 100 simulations, using a different system realization (or sample) in each simulation. The samples are generated by changing the values of R_i, C_i, and r_i of the N nanoscillators according to a random distribution of relative width δ around the specified central values (see Fig. 1(b)). The cases $\delta = 0$ (identical R-SETs, no variability) and $\delta = 0.25$ (significant network variability) are considered. For a given potential V_0, the total number of spikes generated by the network during a fixed time interval τ is divided by the number of nanoscillators $N = 100$ and by the time τ to obtain

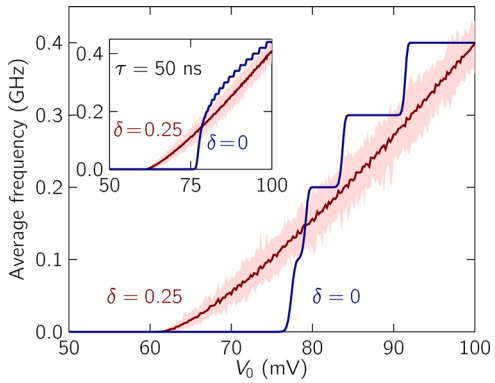

FIG. 2. (Color online) The oscillation frequency of a network of $N = 100$ R-SETs at 5 K with $V_{th} = e/(2C) \approx 80$ mV and $\tau = 10$ ns depends on the applied potential. The lines are the average values of 100 simulations using different network realizations, and the shaded regions span between the maximum and minimum frequencies obtained in these simulations. The cases $\delta = 0$ and $\delta = 0.25$ are considered. The inset shows the effect of increasing τ to 50 ns.

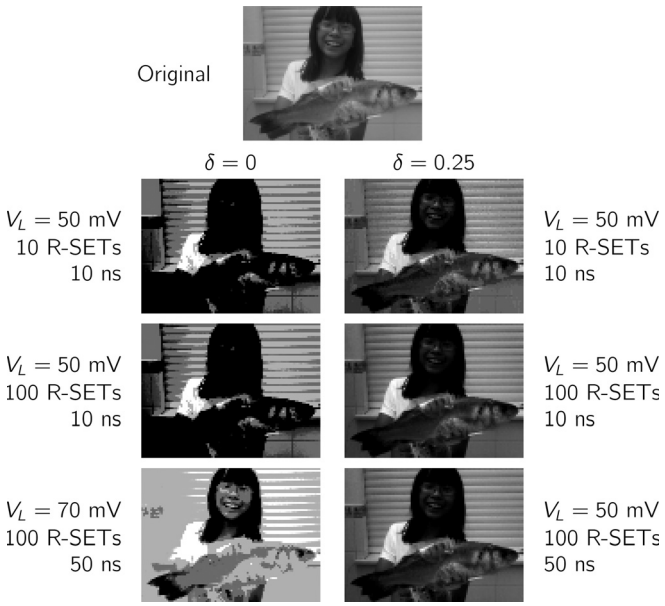

FIG. 3. Every pixel in the original 8-bit image is analyzed with the homogeneous ($\delta = 0$) and heterogeneous ($\delta = 0.25$) networks and the network oscillation frequency is calculated. The output 8-bit image is formed by converting frequencies to gray levels, associating the minimum frequency with a black pixel. The choice $V_L < V_{th} \approx 80$ mV is appropriate for the weak signal regime considered here. The network variability results in an enhanced image transduction that can be further improved by increasing N (from 10 to 100) and τ (from 10 to 50 ns).

the average frequency per nanoscillator (see Fig. 2). The time τ for each simulation is 10 ns, and the inset of Fig. 2 shows the effect of increasing τ to 50 ns. The shaded regions give the uncertainty caused by the variability in the electrical parameters of the R-SETs and the finite temperature $T = 5$ K. At high temperatures, the random nature of tunneling makes it inefficient for the signal processing for the particular range of system parameters considered here. Nevertheless, changes in the values of the tunneling resistances and capacitances of the SET may lead to operation temperatures close to ambient conditions.[18,19,21,23] In particular, significantly higher temperatures can be achieved if we decrease the capacitance by reducing the NP size and using organic ligands with low effective electrical permittivities.[19–25] It is possible to obtain experimentally NP capacitances in the subattofarad regime,[20–23] which opens the door to obtain Coulomb blockade effects similar to those invoked here at higher temperatures.[18,19,21,23] In particular, Coulomb blockade phenomena in ligand-stabilized Au NPs with a core diameter of 1.8 nm have recently been observed in the current–voltage curves of the chemisorbed Au NPs by scanning tunneling spectroscopy at room temperature.[23]

The oscillations of the network of identical R-SETs ($\delta = 0$) only occur when the applied potential V_0 approaches the common threshold potential $V_{th} \approx 80$ mV (see Fig. 2). However, when $\delta > 0$, those nanostructures having lower threshold potentials than the central value ($V_{th,i} < V_{th}$) start oscillating when the applied potential V_0 is in the range $V_{th,i} < V_0 < V_{th}$. Figure 2 shows clearly that the network composed by non-identical units operates over a wider dynamic range than the homogeneous one,[9,12,15] thus providing a more gradual response which can be exploited in image processing involving weak signals.[10,11]

Figure 2 shows that an ensemble of single-electron nanoscillators can transduce potentials into pulses whose frequency is proportional to the amplitude of the input signal (see also Refs. 9 and 15, and references therein). The dependence of the network spike frequency, averaged over all the individual R-SETs, on the potential V_0 permits the transduction of the input potentials (the gray levels of the pixels in Fig. 1(a)) into oscillation frequency outputs (the network rhythms).

Figure 3 shows the results of the frequency-based processing of a 100×75 pixels, 8-bit grayscale digital image using homogeneous and heterogeneous networks of R-SETs. The pixels are analyzed sequentially. For every pixel, the potential applied to the network is $V_0 = g(V_H - V_L) + V_L$, where $V_L = 50$ mV, $V_H = 100$ mV, and g ($0 \le g \le 1$) is the gray level of the pixel, where $g = 0$ corresponds to black. For every pixel, the output is the average frequency of the network, which is converted to a new 8-bit gray level by dividing the frequency of every pixel by the maximum frequency observed (which corresponds to white pixels). It is important to notice that the procedure followed to obtain the results of Fig. 3 is not intended to optimize the image transduction but rather to show the different behavior of the homogeneous and heterogeneous networks for the case of subthreshold signals, i.e., $V_L < V_{th} \approx 80$ mV. Figure 3 shows that the network variability provides a better image transduction than that observed with the identical R-SETs. The image transduction can be further improved for $\delta > 0$ with a moderate increase in the network redundancy N (this effect is not observed for $\delta = 0$) and the simulation time τ. A significant improvement in the image transduction by the homogeneous network requires increasing the minimum potential V_L and the simulation time (see Figs. 2 and 3). Some optimization in the image transduction process could also be achieved in the case of the heterogeneous network by choosing appropriate values of δ and V_L because of the diversity-induced stochastic resonance (see Refs. 10–12, 26, 27, and references therein for the effects of stochastic resonance and dithering phenomena on image perception with noisy neurons). However, the effects caused by the optimization process in the heterogeneous network performance are not as dramatic as those

observed in the homogeneous network for the case of weak signals (see Fig. 3). The heterogeneous network does not depend critically on the external tuning of parameters which is required in the case of the homogenous network because of the diversity in the individual threshold responses of many non-identical units.

In summary, the evidence that variability effects play a significant role in the processing of weak electrical signals by biological threshold units[2–6,28–30] suggests that this variability can also be used to enhance signal processing by artificial nanostructures. We have considered this question here for the case of single-electron oscillators composed by a metallic NP functionalized with organic ligands. We have exploited two physical properties that have been shown to be robust over a wide range of system parameters:[9–12,15] (1) the nanoscillators can transduce potentials into pulses whose frequency is proportional to the amplitude of the input signal and (2) a network composed by non-identical processing units can operate over a wider dynamic range than a homogeneous network. The extension of this work to image recognition after learning is under consideration.

Importantly, the artificial nanostructures in the network of Fig. 1(a) are moderate in number and do not have complex interconnections between them. These facts suggest that signal processing can be possible not only by assembling many nanostructures with complex local interconnections but also by exploiting the variability inherent to the fabrication procedures at the nanoscale in relatively simple architectures. Recent experiments show that coding processes in neuronal populations may not simply be the product of adding more neurons or increasing the number of local connections but also depend on the emerging properties of summing networks composed by a finite number of biologically diverse elements showing nonlinear responses.[4]

The results presented are not just another application of variability-induced phenomena[9–11,15] to the case of a frequency-based transduction scheme. The basic concepts invoked (diversity, oscillating networks, noise, threshold responses, and spike frequencies) are characteristic of signal processing in many biological systems[2–8,28,29] and then can be of interest for exchanging ideas between multidisciplinary fields.

Financial support from the Ministry of Science and Innovation of Spain (project MAT2009-07747) is acknowledged.

[1]J. Pineda de Gyvez and H. P. Tuinhout, IEEE J. Solid-State Circuits **39**, 157 (2004).
[2]J. McGuinness and B. P. Graham, BMC Neurosci. **12**(1), 127 (2011).
[3]Y. Yarom and J. Hounsgaard, Physiol. Rev. **91**, 917 (2011).
[4]K. Padmanabhan and N. N. Urban, Nat. Neurosci. **13**, 1276 (2010).
[5]R. B. Stein, E. R. Gossen, and K. E. Jones, Nat. Rev. Neurosci. **6**, 389 (2005).
[6]J. A. White, J. T. Rubinstein, and A. R. Kay, Trends Neurosci. **23**, 131 (2000).
[7]J. W. Pillow, Y. Ahmadia, and L. Paninski, Neural Comput. **23**, 1 (2011).
[8]S. Schreiber, I. Samengo, and A. V. M. Herz, J. Neurophysiol. **101**, 2239 (2009).
[9]A. K. Kikombo and T. Asai, in *Proceedings of the International Symposium on Intelligent Signal Processing and Communication Systems, Kanazawa, Japan, 2009* (IEEE, Piscataway, NJ, 2009), p. 429.
[10]S. Kasai, K. Miura, and Y. Shiratori, Appl. Phys. Lett. **96**, 194102 (2010).
[11]S. Kasai, in Proceedings of the International Symposium on Intelligent Signal Processing and Communication Systems, Kanazawa, Japan, 2009 (IEEE, Piscataway, NJ, 2009), p. 363.
[12]J. Cervera, J. A. Manzanares, and S. Mafé, Nanoscale **2**, 1033 (2010).
[13]J. Cervera, J. A. Manzanares, and S. Mafé, Nanotechnology **20**, 465202 (2009).
[14]J. Cervera, J. A. Manzanares, and S. Mafé, J. Appl. Phys. **105**, 074315 (2009).
[15]J. Cervera, J. A. Manzanares, and S. Mafé, Nanotechnology **22**, 435201 (2011).
[16]O. Bichler, W. Zhao, F. Alibart, S. Pleutin, D. Vuillaume, and C. Gamrat, IEEE Trans. Electron Devices **57**, 3115 (2010).
[17]D. L. Feldheim and C. D. Keating, Chem. Soc. Rev. **27**, 1 (1998).
[18]K. Luo, D.-H. Chae1, and Z. Yao, Nanotechnology **18**, 465203 (2007).
[19]S. Chen, R. S. Ingram, M. J. Hostetler, J. J. Pietron, R. W. Murray, T. G. Schaaf, J. T. Khoury, M. Alvarez, and R. L. Whetten, Science **20**, 2098 (1998).
[20]R. W. Murray, Chem. Rev. **108**, 2688 (2008).
[21]N. K. Chaki, B. Kakade, K. P. Vijayamohanan, P. Singh, and C. V. Dharmadhikari, Phys. Chem. Chem. Phys. **8**, 1837 (2006).
[22]A. C. Templeton, W. P. Wuelfing, and R. W. Murray, Acc. Chem. Res. **33**, 27 (2000).
[23]S. Kano, Y. Azuma, M. Kanehara, T. Teranishi, and Y. Majima, Appl. Phys. Express **3**, 105003 (2010).
[24]V. Garcia-Morales and S. Mafé, J. Phys. Chem. C **111**, 7242 (2007).
[25]J. Cervera and S. Mafé, J. Nanosci. Nanotechnol. **11**, 7537 (2011).
[26]F. Chapeau-Blondeau, *Noise, Oscillators, and Algebraic Randomness: From Noise in Communication Systems to Number Theory*, edited by M. Planat (Springer, Berlin, 2000), p. 137.
[27]B. Kosko and S. Mitaim, Neural Networks **16**, 755 (2003).
[28]M. J. Barber and M. L. Ristig, Phys. Rev. E **47**, 041913 (2006).
[29]S. M. Bezrukov and I. Vodyanoy, Biophys. J. **73**, 2456 (1997).
[30]J. A. Manzanares, J. Cervera, and S. Mafé, Appl. Phys. Lett. **99**, 153703 (2011).